ACS OMEGA

Article

Cite This: ACS Omega 2019, 4, 12385−12392

http://pubs.acs.org/journal/acsodf

^{11}B NMR Chemical Shift Predictions via Density Functional Theory and Gauge-Including Atomic Orbital Approach: Applications to Structural Elucidations of Boron-Containing Molecules

Peng Gao,[†,‡] Xingyong Wang,[†,‡] Zhenguo Huang,[§] and Haibo Yu*[,†,‡,∥]

[†]School of Chemistry and Molecular Bioscience and [‡]Molecular Horizons, University of Wollongong, Wollongong, New South Wales 2500, Australia

[§]School of Civil and Environmental Engineering, University of Technology Sydney, Sydney, New South Wales 2007, Australia

[∥]Illawarra Health and Medical Research Institute, Wollongong 2522, Australia

Supporting Information

ABSTRACT: ^{11}B nuclear magnetic resonance (NMR) spectroscopy is a useful tool for studies of boron-containing compounds in terms of structural analysis and reaction kinetics monitoring. A computational protocol, which is aimed at an accurate prediction of ^{11}B NMR chemical shifts via linear regression, was proposed based on the density functional theory and the gauge-including atomic orbital approach. Similar to the procedure used for carbon, hydrogen, and nitrogen chemical shift predictions, a database of boron-containing molecules was first compiled. Scaling factors for the linear regression between calculated isotropic shielding constants and experimental chemical shifts were then fitted using eight different levels of theory with both the solvation model based on density and conductor-like polarizable continuum model solvent models. The best method with the two solvent models yields a root-mean-square deviation of about 3.40 and 3.37 ppm, respectively. To explore the capabilities and potential limitations of the developed protocols, classical boron−hydrogen compounds and molecules with representative boron bonding environments were chosen as test cases, and the consistency between experimental values and theoretical predictions was demonstrated.

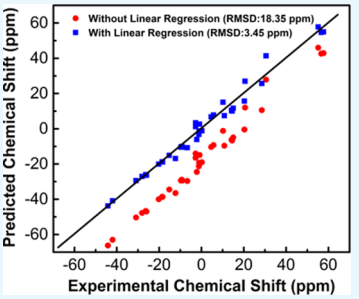

1. INTRODUCTION

The electron deficiency of boron enables fascinating chemistry. The studies of the structure and reactivity of boron-containing molecules have formed the basis of many important chemical concepts.[1] Over the years, boron containing compounds have found a wide range of applications in metallomimetic chemistry,[2] materials science,[3−5] and medicinal chemistry.[6,7] The rapid development of boron chemistry is tightly coupled with the application of ^{11}B nuclear magnetic resonance (NMR) spectroscopy, which has been proved to be one of the most reliable and efficient methods for structural elucidation.[8−10] Such an analysis enables effective elucidations of the chemical environment of boron within a molecule, structural assignments of possible intermediate states, as well as kinetics analysis of the reactions of interest.[11] ^{11}B NMR chemical shift analysis helps convincingly in structural assignment, particularly in the cases for which the X-ray crystallography study is challenging. For instance, Marwitz et al. reported the first isolation and characterization of 1,2-dihydro-1,2-azaborine, a hybrid organic/inorganic benzene isoelectronic structure through NMR analysis.[12] Recently, by monitoring the temperature-dependent ^{11}B chemical shifts, we have conclusively demonstrated that ammonium aminodiboranate, a long-sought isomer of diammoniate of diborane and ammonia borane dimer, is stable at −18 °C and decomposes at elevated temperatures.[13]

The development of various computational methods for chemical shift predictions further improves the capabilities of NMR spectroscopy in structural assignments.[8,14−18] With the introduction of density functional theory (DFT)[19−23] and gauge-including atomic orbital (GIAO)-based approach,[24] the calculations of boron isotropic shielding constants become accessible. At the same time, the application of linear regression correlating calculated isotropic shielding constants and experimental NMR values has also proved effective to improve the prediction accuracy for ^{1}H, ^{13}C, and ^{15}N chemical shifts at relatively low computational costs.[25−30] The linear regression between computed isotropic shielding constants (σ) and experimental chemical shifts (δ) was performed via the following equation

$$\delta = \frac{\text{intercept} - \sigma}{-\text{slope}} \quad (1)$$

There are two empirical scaling factors that need to be fitted: slope and intercept. The former is a correction to the systematic error (the ideal value is −1), whereas the latter corresponds to the choice of reference applied in the NMR measurement. Through these two scaling factors, the

Received: May 28, 2019
Accepted: July 8, 2019
Published: July 19, 2019

Table 1. The Eight Methods Adopted for Calculating ^{11}B Isotropic Shielding Constants and the Fitted Empirical Scaling Parameters (Slope and Intercept) in THF

			SMD[c]		CPCM[d]	
method	geometry[a] (opt & freq)	NMR[b] (GIAO)	slope	intercept	slope	intercept
1	B3LYP/6-31+G(d,p)	mPW1PW91/6-311+G(2d,p)	−1.0869	106.19	−1.0851	106.02
2	B3LYP/6-311+G(2d,p)	mPW1PW91/6-311+G(2d,p)	−1.0877	106.40	−1.0867	106.25
3	B3LYP/6-31+G(d,p)	PBE0/6-311+G(2d,p)	−1.0959	106.32	−1.0941	106.15
4	B3LYP/6-311+G(2d,p)	PBE0/6-311+G(2d,p)	−1.0967	106.53	−1.0956	106.37
5	M062X/6-31+G(d,p)[g]	mPW1PW91/6-311+G(2d,p)	−1.1050	106.67	−1.0903	106.65
5′	M062X/6-31+G(d,p)[g]	mPW1PW91/6-311+G(2d,p)	−1.1170[e]	107.52[e]	−1.1386[f]	107.76[f]
6	M062X/6-311+G(2d,p)[g]	mPW1PW91/6-311+G(2d,p)	−1.1014	106.94	−1.1003	106.79
7	B3LYP/cc-pVDZ	B3LYP/cc-pVDZ	−1.0104	110.96	−1.0078	110.79
7′	B3LYP/cc-pVDZ	B3LYP/cc-pVDZ	−1.0386[e]	111.96[e]	−1.0442[f]	111.80[f]
8	B3LYP/cc-pVTZ	B3LYP/cc-pVTZ	−1.0824	103.20	−1.0823	103.09

[a]The geometry optimization and vibrational frequency calculations were performed with this method. [b]The GIAO calculations[24] were performed with this method together with the implicit solvent models in Gaussian 09. [c]The fitted empirical scaling factors (slope and intercept in eq 1) for the chemical shift calculations with the SMD model.[32] The linear fitting is shown in Figure 1. [d]The fitted empirical scaling factors (slope and intercept in eq 1) for the chemical shift calculations with the CPCM model.[33] The linear fitting is shown in Figure S2 in the Supporting Information. [e]The fitted empirical scaling factors (slope and intercept in eq 1) for the chemical shift calculations with the SMD model included in the optimization step. The linear fitting can be seen in Figure S3 in the Supporting Information. [f]The fitted empirical scaling factors (slope and intercept in eq 1) for the chemical shift calculations with the CPCM model included in the optimization step. The linear fitting can be seen in Figure S3 in the Supporting Information. [g]int=ultrafine was included in all calculations with the M06 functionals.

calculated isotropic shielding constants can be converted into chemical shifts with sufficient accuracy, for instance, to allow distinguishing between different stereoisomers.[29]

In this work, effective predictions of ^{11}B NMR chemical shifts based on linear regression were investigated. First, a database of boron-containing molecules was constructed. Second, we conducted calculations of boron isotropic shielding constants via eight different levels of theory along with two implicit solvent models for comparison. To be consistent with the experimental data, tetrahydrofuran (THF) was included as the solvent in our calculations. Third, the corresponding linear regression scaling factors were derived, and the ones with the best performance were subjected to further tests on a diverse set of boron-containing molecules including a series of boron−hydrogen compounds. Together with the previous work on ^{1}H,[25,26] ^{13}C,[26,30,31] and ^{15}N,[28,29,31] accurate NMR chemical shift predictions for molecules containing these elements can be achieved.

2. RESULTS AND DISCUSSIONS

2.1. The Performance of the Adopted Methods. The fitted empirical scaling factors are listed in Table 1, and their performances are summarized in Table 2. The linear regressions are shown in Figure 1. For all eight methods with implicit solvent models, the values of R^2 were close to 1.0 (Table 1), indicating that the applied data are suitable for linear regression. At the same time, the deviation of the slope from −1 indicates the existence of systematic errors in the adopted DFT/GIAO-based calculations.[26] From the root-mean-square deviation (RMSD) values, we can see that all eight methods performed reasonably well. By the linear regression, they predicted ^{11}B chemical shifts with errors of 3.40−3.50 and 3.37−3.50 ppm with respect to the experimental data using the solvation model based on density (SMD) and conductor-like polarizable continuum model (CPCM) solvent models, respectively (Table 2 and Figure S2 in the Supporting Information). In contrast, the corresponding errors of the results obtained without linear regression are substantially larger (>18 ppm) (Table 2),

Table 2. The Performance of the Fitted Empirical Scaling Factors for the Eight Methods in Table 1

method	R^2[a]	RMSD[b]	RMSD[c]	R^2[a]	RMSD[b]	RMSD[c]
	SMD			CPCM		
1	0.9812	3.40	19.52	0.9813	3.38	19.41
2	0.9811	3.40	19.18	0.9812	3.40	19.07
3	0.9812	3.40	19.57	0.9813	3.39	19.45
4	0.9811	3.41	19.22	0.9812	3.40	19.11
5	0.9807	3.45	18.35	0.9803	3.48	18.32
5′[d]	0.9796	3.55	18.11	0.9818	3.34	18.49
6	0.9801	3.50	18.10	0.9800	3.50	17.99
7	0.9811	3.41	20.17	0.9815	3.37	20.06
7′[d]	0.9821	3.31	19.51	0.9832	3.21	19.45
8	0.9807	3.45	22.38	0.9808	3.44	22.30

[a]R^2 is the coefficient of determination for the linear regression. [b]RMSD for the predicted chemical shifts of the boron-containing molecules in the database (see Table S1 in the Supporting Information) with respect to their respective experimental values (in ppm) with linear regression. [c]RMSD for the predicted chemical shifts of the boron-containing molecules in the database (see Table S1 in the Supporting Information) with respect to their respective experimental values (in ppm) without linear regression (using BF_3OEt_2 as reference). [d]Implicit solvent models (CPCM or SMD) were included in the optimization step.

demonstrating the effectiveness of the fitted scaling factors in improving prediction accuracy. It is worth noting that the boron atoms bonded with halogen atoms have a large error, which has also been noted in ^{13}C chemical shift predictions and is likely due to the deficiency in the adopted DFT method for this class of compounds.[26]

Based on the above results, it can be seen that all of the eight methods display comparably good performances. PBE0 and mPW1PW91 provide similar accuracy for ^{11}B NMR chemical shift predictions (method 1 vs 3 and 2 vs 4). Method 5 and 7, with geometry optimization at M062X/6-31+G(d,p) or B3LYP/cc-pVDZ in the gas phase and NMR GIAO calculations at mPW1PW91/6-311+G(2d,p) or B3LYP/cc-pVDZ, were proved to be effective for not only ^{11}B, but also for

DOI: 10.1021/acsomega.9b01566
ACS Omega 2019, 4, 12385−12392

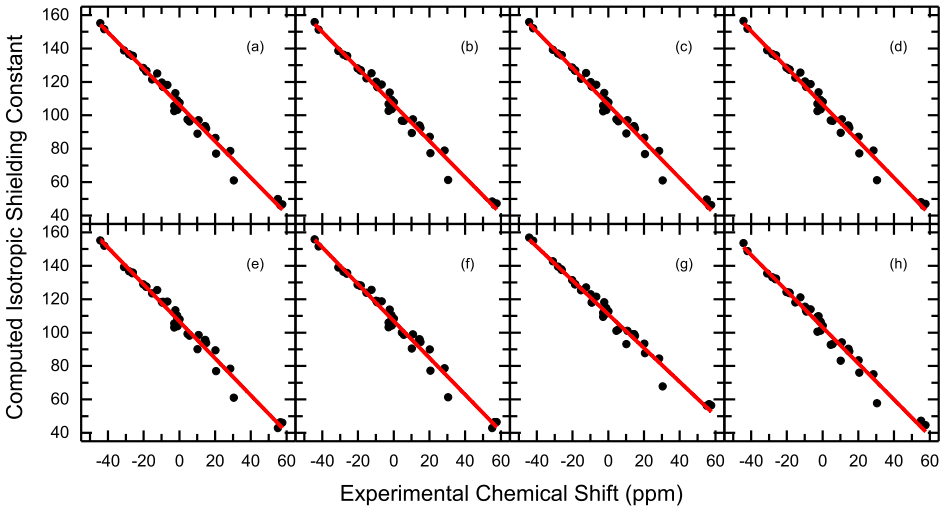

Figure 1. Linear regression between the experimental ^{11}B chemical shifts and calculated isotropic shielding constants with method 1−8 with the SMD solvent model for NMR GIAO calculations. (a) Method 1; (b) method 2; (c) method 3; (d) method 4; (e) method 5; (f) method 6; (g) method 7; and (h) method 8. See Figure S2 in the Supporting Information for more details for the linear regression with the CPCM solvent model for NMR GIAO calculations.

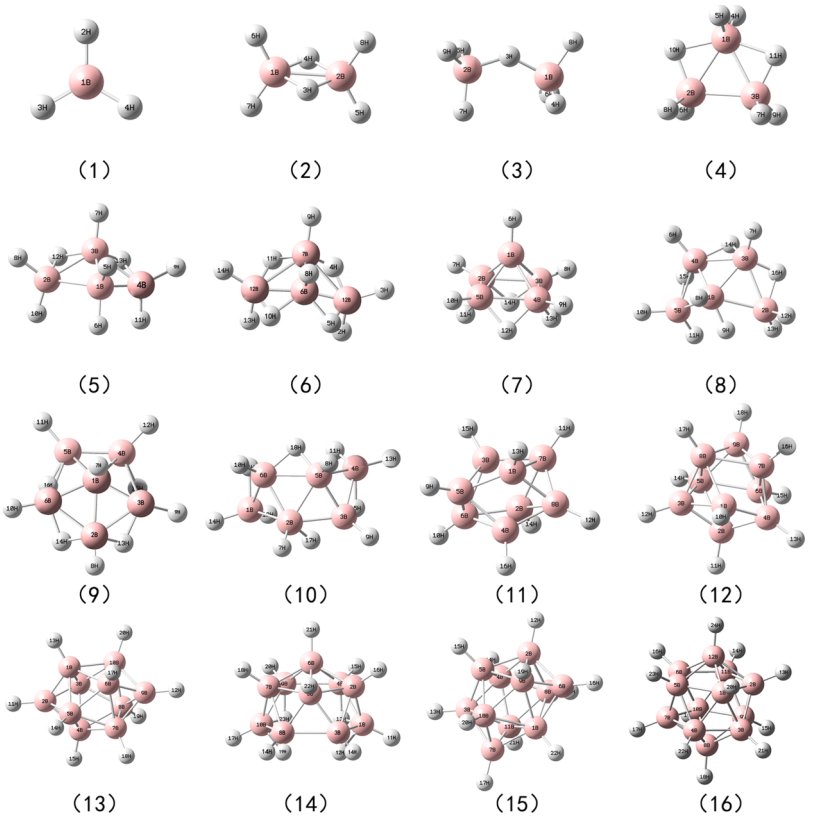

Figure 2. Boron−hydrogen compounds included in the application study.

^{1}H, ^{13}C, and ^{15}N chemical shift predictions as discussed before.[26,28−30] In particular, the important advantage of method 5 (with the SMD solvent model) is that it could provide chemical shift predictions for ^{1}H, ^{13}C, ^{15}N, and ^{11}B with a consistent accuracy in one set of calculation via the corresponding changes of the applied solvents.[27,29]

For the two implicit solvent models (SMD and CPCM), we found that their prediction errors of ^{11}B NMR chemical shifts are very similar (Table 2). Moreover, we investigated the potential benefit of including the implicit solvent models in the geometry optimization (method 5′ and 7′ in Table 2 and Figure S3 in the Supporting Information) in contrast to those in vacuo (method 5 and 7). Only minor changes were observed (RMSD changes less than 0.15 ppm), indicating that the inclusion of implicit solvent models in geometry optimization may not improve the result significantly. Specifically, for the SMD model, the prediction error for method 5′ increases slightly from 3.45 to 3.55 ppm, whereas the error decreases from 3.41 to 3.31 ppm with method 7′. The result obtained with the CPCM model shows a slight

DOI: 10.1021/acsomega.9b01566
ACS Omega 2019, 4, 12385−12392

Table 3. Experimental and Predicted ^{11}B NMR Chemical Shifts (in ppm) for Selected Boron−Hydrogen Compounds[a]

			$\delta_{pred.}$			
	Pos.[b]	Exp.[c]	5[d]	7[e]	5[f]	7[g]
BH_3	$\delta_{B\text{-}1}$	86.0	84.22	83.16	85.34	83.20
B_2H_6	$\delta_{B\text{-}1,2}$	16.6	17.84	15.98	18.06	15.85
$B_2H_7^-$	$\delta_{B\text{-}1,2}$	−24.6	−24.51	−23.48	−24.86	−23.71
$B_3H_8^-$	$\delta_{B\text{-}1\text{-}3}$	−30.4	−26.99[h]	−28.16[h]	27.37[h]	28.40[h]
$B_4H_9^-$	$\delta(1)_{B\text{-}1}$	−54.5	−54.41	−56.46	−55.16	−56.77
	$\delta(2)_{B\text{-}2,4}$	−10.2	−11.65	−12.72	−11.83	−12.92
	$\delta(3)_{B\text{-}3}$	0.8	0.06	−1.41	0.05	−1.58
B_4H_{10}	$\delta(1)_{B\text{-}6,7}$	−6.9	−6.85	−7.51	−6.97	−7.70
	$\delta(2)_{B\text{-}12}$	−41.8	−40.18	−42.75	−40.74	−43.03
B_5H_9	$\delta(1)_{B\text{-}1}$	−13.4	−14.17	−15.47	−14.38	−15.68
	$\delta(2)_{B\text{-}2\text{-}5}$	−53.1	−50.65	−55.75	−51.35	−56.06
B_5H_{11}	$\delta_{B\text{-}1\text{-}5}$	−55.3	−51.38	−53.43	−52.09	−53.74
B_6H_{10}	$\delta(1)_{B\text{-}3\text{-}6}$	18.6	14.77	14.98	14.95	14.85
	$\delta(2)_{B\text{-}2}$	−6.5	−8.23	−11.13	−8.36	−11.33
	$\delta(3)_{B\text{-}1}$	−51.8	−48.95	−51.64	−49.63	−51.94
B_6H_{12}	$\delta(1)_{B\text{-}1,4}$	22.6	22.56	20.43	22.85	20.32
	$\delta(2)_{B\text{-}3,6}$	7.9	11.04	10.15	11.17	10.01
$B_8H_8^{2-}$	$\delta_{B\text{-}1\text{-}8}$	−6.8	−1.55	−3.60	−1.59	−3.78
$B_9H_9^{2-}$	$\delta(1)_{B\text{-}3,4,9}$	−2.9	−3.60	−6.40	−3.67	−6.59
	$\delta(2)_{B\text{-}1,2,5\text{-}8}$	−20.5	−21.98	−22.22	−22.30	−22.45
$B_{10}H_{10}^{2-}$	$\delta(1)_{B\text{-}1,3\text{-}8,10}$	−30.9	−28.38	−28.85	−28.78	−29.10
	$\delta(2)_{B\text{-}2,9}$	0.9	−2.47	−3.18	−2.52	−3.36
$B_{10}H_{14}$	$\delta(1)_{B\text{-}5,6}$	13.5	12.66	12.20	12.81	12.06
	$\delta(2)_{B\text{-}1,10}$	10.7	8.18	7.62	8.27	7.47
	$\delta(3)_{B\text{-}3,4,8,9}$	1.6	0.65	0.42	0.64	0.25
	$\delta(4)_{B\text{-}2,7}$	−35.2	−33.14	−34.95	−33.60	−35.21
$B_{11}H_{11}^{2-}$	$\delta_{B\text{-}1\text{-}11}$	−16.9	−17.10	−17.63	−17.35	−17.85
$B_{12}H_{12}^{2-}$	$\delta_{B\text{-}1\text{-}12}$	−15.6	−13.82	−14.62	−14.03	−14.83

[a]All of the NMR calculations were conducted in vacuo. [b]Positions for the boron of interest, more details can be seen in Table S6 in Supporting Information. [c]Experimental data were taken from refs.[37,41,46−49] [d]The predicted chemical shifts via the linear regression model by method 5 (the SMD set). [e]The predicted chemical shifts via the linear regression model by method 7 (the SMD set). [f]The predicted chemical shifts via the linear regression model by method 5 (the CPCM set). [g]The predicted chemical shifts via the linear regression model by method 7 (the CPCM set). [h]For $B_3H_8^-$, our calculations predicted two different chemical shifts for boron atoms, and the averaged value was used to compare with the experimental value.

difference, where the errors for both method 5 and 7 decrease. Considering their increased computational costs and the corresponding gain in accuracy, we recommend to use gas phase geometry optimization and only include the solvent model for the NMR calculation step.

2.2. Applications of ^{11}B Chemical Shift Predictions for Boron−Hydrogen Compounds. We applied the developed protocol to illustrate its possible assistance for experimental work in the field of hydrogen storage. In recent years, because of the high content of hydrogen,[34,35] the studies of boron−hydrogen compounds have attracted increasing interest from the community of hydrogen storage. Nevertheless, effective identification of the intermediates during hydrogen evolution remains a challenge. From the perspective of the NMR analysis, merely relying on ^{1}H NMR spectroscopy is not sufficient.[36] Combining ^{1}H and ^{11}B NMR spectroscopies can be a powerful strategy in resolving the structure of boron−hydrogen compounds.

In this study, we tested 16 classical boron−hydrogen compounds (Figure 2), for which experimental data are available (Table 3). We conducted the NMR GIAO calculations via method 5 and 7 in vacuo following the same procedure as above. Table 3 and Figure 3 show an excellent agreement between the predicted values and experimental data.[37] For both method 5 and 7, scaling factors derived from both SMD and CPCM models work equally well, and most of the prediction errors are within 1.0 RMSD.

The diborane, B_2H_6, which has two bridging hydrogen atoms and features a ring structure (structure **2** in Figure 2), is a highly reactive reagent that has versatile applications. As can be seen from Figure 2, the optimized structure shows a planar ring of diborane with the dihedral angle between H_b−B−H_b−B at 0°, matching well with the experimental measurement[38,39] and previous computational work.[37] The deviations of the predicted values from the experimental data are within 1.5 ppm. The anion $B_3H_8^-$ (structure **4** in Figure 2) has attracted a lot of attention due to its stability and high content of hydrogen.[40,41] This anion may adopt different structures in solution.[42] Indeed, solution NMR studies have shown that the transformation between possible structures can happen via the migration of hydrogen.[43−45] Considering the fluxional behavior of $B_3H_8^-$, we applied the same procedure by Sethio et al.[37] to average the two predicted values of ^{11}B NMR chemical shifts, and then compare the average with experimental data. From Table 3, we found that the deviations are within 3.4 and 2.2 ppm for method 5 and 7, respectively, which is in a reasonable agreement with the experimental data. In contrast, Sethio et al.

DOI: 10.1021/acsomega.9b01566
ACS Omega 2019, 4, 12385−12392

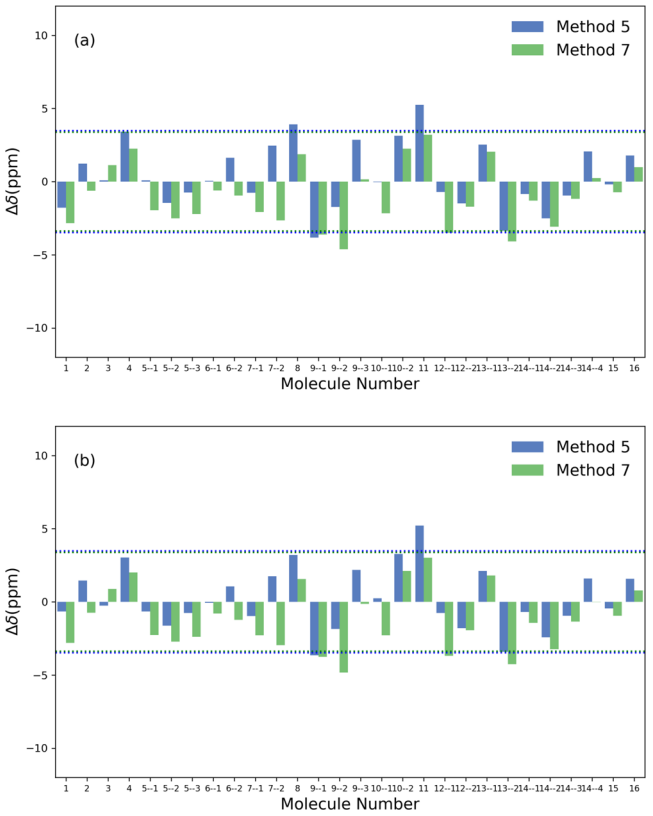

Figure 3. The deviations between the predicted and experimental ^{11}B NMR chemical shifts of molecules listed in Table 3. (a) The isotropic shielding constants were calculated with method 5 and 7 with the SMD model, and were converted to chemical shifts with the scaling factors of the SMD set listed in Table 1. The RMSD value is marked by the dashed line. (b) The isotropic shielding constants were calculated with method 5 and 7 with the CPCM model, and were converted to chemical shifts with the scaling factors of the CPCM set listed in Table 1. The RMSD value is marked by the dashed line.

reported errors ~6−9 ppm for three different DFT methods without linear regressions.[37]

2.3. Applications of ^{11}B Chemical Shift Predictions for Structural Elucidations of Boron Containing Molecules. We also applied our protocol to further test some other boron containing molecules with diverse bonding environments and investigate their overall applicability (Figure 4). From the results listed in Table 4 and deviations shown in Figure 5, we can see that the agreement between the predicted values and experimental data is excellent, indicating the robustness of our protocol for structural elucidations of boron containing molecules with different bonding features. It is worth pointing out that, some of these experimental ^{11}B chemical shift values were measured in pure liquids or solvents other than THF (Table 4). We infer that there exists a reasonable transferability for scaling factors among different solvents. This is consistent with our previous work on nitrogen NMR chemical shift predictions.[29]

3. METHODOLOGY

3.1. Database of Boron-Containing Molecules. There are 36 molecules and 36 chemical shifts in total included in our database (see Table S1 in the Supporting Information for more details). The two criteria for selection of molecules include (a) reliable experimental data available, preferably in THF;[50] and

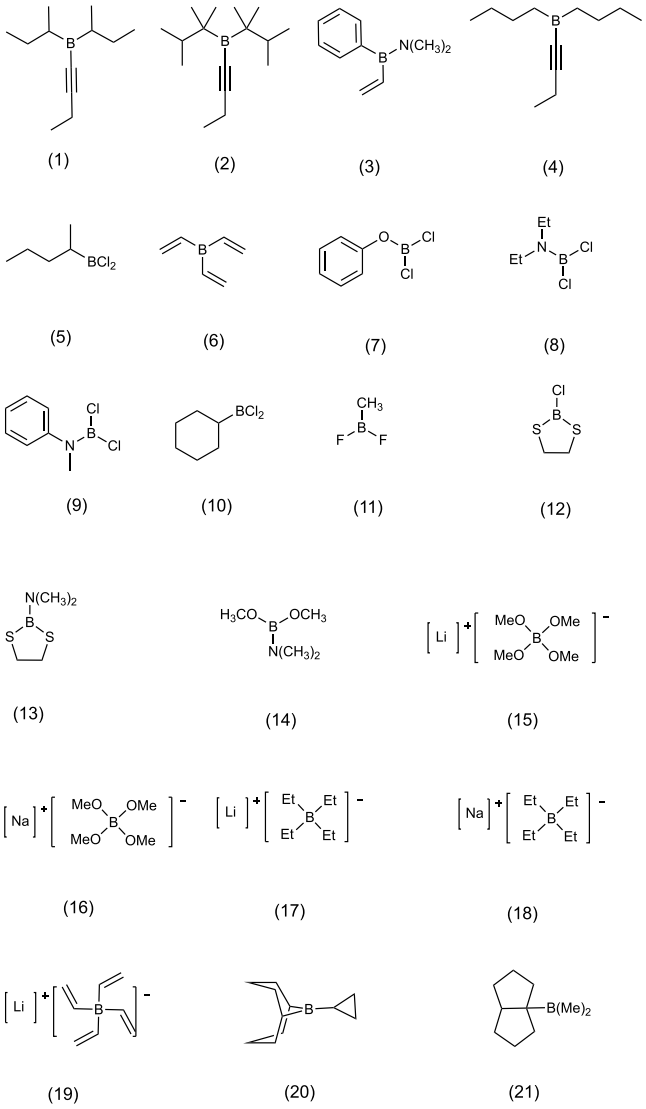

Figure 4. Boron containing molecules included in the application study.

(b) having relatively rigid boron skeletons. As discussed in ref 29, the reason for the second criterion is to avoid the potential challenges in dealing with flexible molecules when developing linear regression models, which require Boltzmann averaging of the calculated isotropic shielding constants on the basis of relative energies of all available conformers. However, the developed scaling factors are expected to be applicable for flexible molecules, provided that the relative energies of their relevant conformers can be calculated accurately.[26]

3.2. Computational Details. To be consistent with the procedure proposed by Tantillo and co-workers[26,27] and our previous study on ^{15}N NMR chemical shifts,[29] we first carried out geometry optimization in vacuo to locate the minima on the potential energy surface. These optimized structures were verified by vibrational frequency calculations. Second, we conducted NMR single-point calculations in THF with both the SMD[32] and CPCM[33] solvent models. It has been shown that the inclusion of the implicit solvent model in the NMR calculation step is crucial to improve the prediction accuracy of ^{1}H and ^{13}C chemical shifts.[25−27] Another study by Xin et al. focusing on ^{13}C chemical shift predictions adopted the CPCM solvent model.[30] The inclusion of the explicit solvent model

DOI: 10.1021/acsomega.9b01566
ACS Omega 2019, 4, 12385−12392

Table 4. Experimental and Predicted ^{11}B NMR Chemical Shifts (in ppm) for Selected Boron Containing Molecules[a]

	Exp.[b]	5[c]	7[d]	5[e]	7[f]
		$\delta_{pred.}$			
1	72.2	67.32	67.89	68.22	67.94
2	81.1	76.99	81.02	78.67	81.83
3	40.0	37.88	38.83	38.38	38.76
4	72.0	66.94	66.90	67.82	66.90
5	65.3	61.98	64.78	62.80	64.77
6	55.2	51.21	51.06	51.88	51.02
7	33.0	32.72	31.82	33.14	31.74
8	31.6	31.76	33.38	32.17	33.29
9	30.8	32.31	32.69	32.73	32.60
10	67.6	61.37	64.30	62.18	64.30
11	28.1	30.43	25.27	30.85	25.16
12	62.7	59.53	62.98	60.32	62.97
13	45.3	43.30	45.44	43.86	45.39
14	21.3	21.10	17.71	21.37	17.59
15	3.0	3.51	1.23	3.52	1.06
16	2.7	3.07	0.86	3.11	0.72
17	−17.5	−17.29	−17.03	−17.41	−17.07
18	−16.6	−18.08	−17.92	−18.25	−18.10
19	−16.1	−12.91	−12.52	−13.19	−12.79
20	84	79.37	80.94	80.591	81.29
21	82.3	80.70	77.75	82.17	78.24

[a]Details of the calculations can be found in Tables S9 and S10 in the Supporting Information. [b]Experimental data.[50] [c]The difference between experimental values and calculated chemical shifts with the linear regression model by method 5 (the SMD set). [d]The difference between experimental values and calculated chemical shifts with the linear regression model by method 7 (the SMD set). [e]The difference between experimental values and calculated chemical shifts with the linear regression model by method 5 (the CPCM set). [f]The difference between experimental values and calculated chemical shifts with the linear regression model by method 7 (the CPCM set).

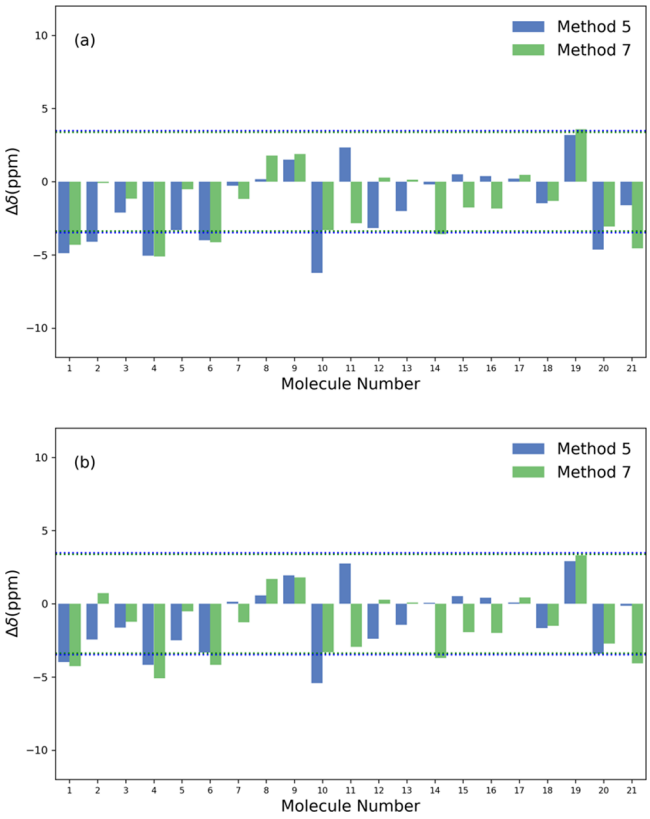

Figure 5. The deviations between the predicted and experimental ^{11}B NMR chemical shifts of molecules listed in Table 4. (a) Isotropic shielding constants were calculated with methods 5 and 7 with the SMD model and were converted to chemical shifts with the scaling factors of the SMD set listed in Table 1. The RMSD value is marked by the dash. (b) Isotropic shielding constants were calculated with method 5 and 7 with the CPCM model and were converted to chemical shifts with the scaling factors of the CPCM set listed in Table 1. The RMSD value is marked by the dash line.

may further improve the prediction accuracy of chemical shifts,[51,52] with a substantial increase of the computational cost. For consistency with the previous studies,[26−30] implicit solvent models were adopted in the current work. The GIAO approach was applied to calculate ^{11}B isotropic shielding constants.[24] All of the calculations were carried out with Gaussian 09.[53] The first six levels of theory (Table 1, method 1−6) are to follow Tantillo and co-workers' work on ^{1}H and ^{13}C chemical shifts[26,27] and our previous study on ^{15}N chemical shifts.[29] In addition, two methods (Table 1, method 7 and 8), which have been shown to provide accurate predictions for both ^{15}N[28] and ^{13}C[30] chemical shift calculations, were also included for comparison. To further investigate the solvent effects, additional calculations with an implicit solvent model included in the geometry optimization step were carried out for two levels of theory (method 5′ and 7′).

4. CONCLUSIONS

In this study, empirical scaling techniques for accurate prediction of ^{11}B NMR chemical shifts have been proposed by comparing eight different levels of theory with two solvent models, based on the calculated isotropic shielding constants in THF. The protocol of ^{11}B NMR chemical shift prediction is consistent with the procedure proposed by Tantillo and co-workers[26,27] for ^{1}H and ^{13}C chemical shifts and our previous work for ^{15}N chemical shift.[29] The two sets of scaling factors for two different solvent models (SMD and CPCM) were compared. Among the eight levels of theory, method 5 and 7 show the best performance, with geometry optimization in the gas phase at M062X/6-31+G(d,p) or B3LYP/cc-pVDZ and NMR GIAO calculation at mPW1PW91/6-311+G(2d,p) or B3LYP/cc-pVDZ with an implicit solvent model. At the same time, the effect of including solvent model in the optimization step was also investigated. In summary, we recommend method 5 and 7 for ^{11}B chemical shift prediction together with those for ^{1}H, ^{13}C, and ^{15}N in one set of calculations. For boron−hydrogen compounds or other boron-containing molecules, the predicted ^{11}B chemical shifts with method 5 and 7 agree well with the experimental data, indicating the robustness and broad applicability of this protocol for structural elucidation. It is worth noting that the fitted scaling factors in THF can provide a reasonable prediction for ^{11}B chemical shifts measured in either pure liquids or in other solvents. This is consistent with the finding of our previous research on ^{15}N chemical shift.[29] We expect that this work on ^{11}B chemical shift can serve as a useful tool for elucidating or confirming the structure of boron-containing compounds.

DOI: 10.1021/acsomega.9b01566
ACS Omega 2019, 4, 12385−12392

■ ASSOCIATED CONTENT

Supporting Information

The Supporting Information is available free of charge on the ACS Publications website at DOI: 10.1021/acsomega.9b01566.

Experimental ^{11}B NMR chemical shifts used in this study and figures for linear regression between the experimental ^{11}B NMR chemical shifts and the calculated isotropic shielding constants with the CPCM solvent model (PDF)

■ AUTHOR INFORMATION

Corresponding Author

*E-mail: hyu@uow.edu.au. Phone: +61 (2) 4221 4235. Fax: +61 (2) 4221 4287.

ORCID

Zhenguo Huang: 0000-0003-1985-0884

Haibo Yu: 0000-0002-1099-2803

Notes

The authors declare no competing financial interest.

■ ACKNOWLEDGMENTS

H.Y. is the recipient of an Australian Research Council Future Fellowship (project number FT110100034) and X.W. is the recipient of a University of Wollongong Vice-Chancellor's Postdoctoral Fellowship. We wish to acknowledge the Australian Government for an Australian International Postgraduate Award scholarship for P.G. This research was in part supported under the Australian Research Council's Discovery Projects funding scheme (project number DP170101773). We wish to acknowledge that this research was undertaken with the assistance of resources provided at the NCI National Facility systems at the Australian National University through the National Computational Merit Allocation Scheme supported by the Australian Government (Project id: v15).

■ REFERENCES

(1) Bregadze, V. I.; Xie, Z. Boron Chemistry - A Rapidly Expanding Research Field. *Eur. J. Inorg. Chem.* **2017**, *2017*, 4348−4349.

(2) Légaré, M.-A.; Pranckevicius, C.; Braunschweig, H. Metallomimetic Chemistry of Boron. *Chem. Rev.* **2019**, DOI: 10.1021/acs.chemrev.8b00561, , in press .

(3) Demirci, U.; Miele, P.; Yot, P. Boron-Based (Nano-)Materials: Fundamentals and Applications. *Crystals* **2016**, *6*, 118.

(4) Huang, Z.; Autrey, T. Boron-nitrogen-hydrogen (BNH) compounds: recent developments in hydrogen storage, applications in hydrogenation and catalysis, and new syntheses. *Energy Environ. Sci.* **2012**, *5*, 9257.

(5) Wang, X.; Yu, L.; Inakollu, V. S. S.; Pan, X.; Ma, J.; Yu, H. Molecular Quantum Dot Cellular Automata Based on Diboryl Monoradical Anions. *J. Phys. Chem. C* **2018**, *122*, 2454−2460.

(6) Leśnikowski, Z. J. Challenges and Opportunities for the Application of Boron Clusters in Drug Design. *J. Med. Chem.* **2016**, *59*, 7738−7758.

(7) Issa, F.; Kassiou, M.; Rendina, L. M. Boron in Drug Discovery: Carboranes as Unique Pharmacophores in Biologically Active Compounds. *Chem. Rev.* **2011**, *111*, 5701−5722.

(8) Todd, L. J.; Siedle, A. R. NMR studies of boranes, carboranes and hetero-atom boranes. *Prog. Nucl. Magn. Reson. Spectrosc.* **1979**, *13*, 87−176.

(9) Wrackmeyer, B. Nuclear Magnetic Resonance Spectroscopy of Boron Compounds Containing Two-, Three- and Four-Coordinate Boron. In *Annual Reports on NMR Spectroscopy*; Webb, G., Ed.; Academic Press, 1988; Vol. *20*; pp 61−203.

(10) Siedle, A. ^{11}B NMR Spectroscopy. In *Annual Reports on NMR Spectroscopy*; Webb, G., Ed.; Academic Press, 1988; Vol. *20*; pp 205−314.

(11) Noeth, H.; Wrackmeyer, B. *Nuclear Magnetic Resonance Spectroscopy of Boron Compounds*, 1st ed.; Springer-Verlag: Berlin, Heidelberg, New York, 1978.

(12) Marwitz, A. J. V.; Matus, M. H.; Zakharov, L. N.; Dixon, D. A.; Liu, S.-Y. A Hybrid Organic/Inorganic Benzene. *Angew. Chem.* **2009**, *121*, 991−995.

(13) Chen, W.; Yu, H.; Wu, G.; He, T.; Li, Z.; Guo, Z.; Liu, H.; Huang, Z.; Chen, P. Ammonium Aminodiboranate: A Long-Sought Isomer of Diammoniate of Diborane and Ammonia Borane Dimer. *Chem.—Eur. J.* **2016**, *22*, 7727−7729.

(14) Buhl, M.; Gauss, J.; Hofmann, M.; Schleyer, P. v. R. Decisive electron correlation effects on computed boron-11 and carbon-13 NMR chemical shifts. Application of the GIAO-MP2 method to boranes and carbaboranes. *J. Am. Chem. Soc.* **1993**, *115*, 12385−12390.

(15) Buehl, M.; Von Ragué Schleyer, P. Application and Evaluation of ab Initio Chemical Shift Calculations for Boranes and Carboranes. How reliable Are accurate Experimental Structures? *J. Am. Chem. Soc.* **1992**, *114*, 477−491.

(16) McKee, M. L.; Lipscomb, W. N. Ab initio study of the transient boron hydrides B3H7, B3H9, B4H8, and B4H12 and the fluxional anion B3H8-. *Inorg. Chem.* **1982**, *21*, 2846−2850.

(17) Łodziana, Z.; Bloński, P.; Yan, Y.; Rentsch, D.; Remhof, A. NMR Chemical Shifts of 11B in Metal Borohydrides from First-Principle Calculations. *J. Phys. Chem. C* **2014**, *118*, 6594−6603.

(18) Tian, S. X. Ab Initio and Electron Propagator Theory Study of Boron Hydrides. *J. Phys. Chem. A* **2005**, *109*, 5471−5480.

(19) Kohn, W.; Sham, L. J. Self-Consistent Equations Including Exchange and Correlation Effects. *Physical Review* **1965**, *140*, A1133−A1138.

(20) Becke, A. D. Density-functional thermochemistry. III. The role of exact exchange. *J. Chem. Phys.* **1993**, *98*, 5648−5652.

(21) Perdew, J. P.; Ernzerhof, M.; Burke, K. Rationale for mixing exact exchange with density functional approximations. *J. Chem. Phys.* **1996**, *105*, 9982−9985.

(22) Adamo, C.; Barone, V. Toward reliable density functional methods without adjustable parameters: The PBE0 model. *J. Chem. Phys.* **1999**, *110*, 6158−6170.

(23) Zhao, Y.; Truhlar, D. G. Density Functional for Spectroscopy: No Long-Range Self-Interaction Error, Good Performance for Rydberg and Charge-Transfer States, and Better Performance on Average than B3LYP for Ground States. *J. Phys. Chem. A* **2006**, *110*, 13126−13130.

(24) Ditchfield, R. Self-consistent perturbation theory of diamagnetism. *Mol. Phys.* **1974**, *27*, 789−807.

(25) Jain, R.; Bally, T.; Rablen, P. R. Calculating Accurate Proton Chemical Shifts of Organic Molecules with Density Functional Methods and Modest Basis Sets. *J. Org. Chem.* **2009**, *74*, 4017−4023.

(26) Lodewyk, M. W.; Siebert, M. R.; Tantillo, D. J. Computational Prediction of ^{1}H and ^{13}C Chemical Shifts: A Useful Tool for Natural Product, Mechanistic, and Synthetic Organic Chemistry. *Chem. Rev.* **2012**, *112*, 1839−1862.

(27) CHESHIRE CCAT, the Chemical Shift Repository for computed NMR scaling factors, with Coupling Constants Added Too. 2017, http://cheshirenmr.info/index.htm (accessed May 20, 2019).

(28) Xin, D.; Sader, C. A.; Fischer, U.; Wagner, K.; Jones, P.-J.; Xing, M.; Fandrick, K. R.; Gonnella, N. C. Systematic investigation of DFT-GIAO 15N NMR chemical shift prediction using B3LYP/cc-pVDZ: application to studies of regioisomers, tautomers, protonation states and N-oxides. *Org. Biomol. Chem.* **2017**, *15*, 928−936.

(29) Gao, P.; Wang, X.; Yu, H. Towards an Accurate Prediction of Nitrogen Chemical Shifts by Density Functional Theory and Gauge-Including Atomic Orbital. *Adv. Theory Simul.* **2019**, *2*, 1800148.

DOI: 10.1021/acsomega.9b01566
ACS Omega 2019, 4, 12385−12392

(30) Xin, D.; Sader, C. A.; Chaudhary, O.; Jones, P.-J.; Wagner, K.; Tautermann, C. S.; Yang, Z.; Busacca, C. A.; Saraceno, R. A.; Fandrick, K. R.; Gonnella, N. C.; Horspool, K.; Hansen, G.; Senanayake, C. H. Development of a 13C NMR Chemical Shift Prediction Procedure Using B3LYP/cc-pVDZ and Empirically Derived Systematic Error Correction Terms: A Computational Small Molecule Structure Elucidation Method. *J. Org. Chem.* **2017**, *82*, 5135−5145.
(31) Jaźwiński, J.; Stefaniak, L. Structural studies on mesoionic 1,2,3,4-thiatriazolo-5-aminides and 1,2,3,4-thiatriazolo-5-methylides by nitrogen and carbon NMR. *Magn. Reson. Chem.* **1993**, *31*, 447−450.
(32) Marenich, A. V.; Cramer, C. J.; Truhlar, D. G. Universal Solvation Model Based on Solute Electron Density and on a Continuum Model of the Solvent Defined by the Bulk Dielectric Constant and Atomic Surface Tensions. *J. Phys. Chem. B* **2009**, *113*, 6378−6396.
(33) Barone, V.; Cossi, M. Quantum Calculation of Molecular Energies and Energy Gradients in Solution by a Conductor Solvent Model. *J. Phys. Chem. A* **1998**, *102*, 1995−2001.
(34) Züttel, A.; Borgschulte, A.; Orimo, S.-I. Tetrahydroborates as new hydrogen storage materials. *Scr. Mater.* **2007**, *56*, 823−828.
(35) Orimo, S.-i.; Nakamori, Y.; Eliseo, J. R.; Züttel, A.; Jensen, C. M. Complex Hydrides for Hydrogen Storage. *Chem. Rev.* **2007**, *107*, 4111−4132.
(36) Hwang, S.-J.; Bowman, R. C.; Reiter, J. W.; Rijssenbeek; Soloveichik, G. L.; Zhao, J.-C.; Kabbour, H.; Ahn, C. C. NMR Confirmation for Formation of [B12H12]2-Complexes during Hydrogen Desorption from Metal Borohydrides. *J. Phys. Chem. C* **2008**, *112*, 3164−3169.
(37) Sethio, D.; Lawson Daku, L. M.; Hagemann, H. A theoretical study of the spectroscopic properties of B2H6 and of a series of BxHyz-species (x=1-12, y=3-14, z=0-2): From BH3 to $B12H12^{-2}$. *Int. J. Hydrogen Energy* **2016**, *41*, 6814−6824.
(38) Duncan, J. L.; Harper, J. The structure of the diborane molecule. *Mol. Phys.* **1984**, *51*, 371−380.
(39) Bartell, L. S.; Carroll, B. L. Electron-Diffraction Study of Diborane and Deuterodiborane. *J. Chem. Phys.* **1965**, *42*, 1135−1139.
(40) Huang, Z.; Lingam, H. K.; Chen, X.; Porter, S.; Du, A.; Woodard, P. M.; Shore, S. G.; Zhao, J.-C. Synthesis, structural analysis, and thermal decomposition studies of [(NH3)2BH2]B3H8. *RSC Adv.* **2013**, *3*, 7460−7465.
(41) Yan, Y.; Remhof, A.; Rentsch, D.; Lee, Y.-S.; Whan Cho, Y.; Züttel, A. Is Y2(B12H12)3 the main intermediate in the decomposition process of Y(BH4)3? *Chemical Communications* **2013**, *49*, 5234−5236.
(42) Olson, J. K.; Boldyrev, A. I. Ab initio characterization of the flexural anion found in the reversible dehydrogenation. *Comput. Theoret. Chem.* **2011**, *967*, 1−4.
(43) Bushweller, C. H.; Beall, H.; Grace, M.; Dewkett, W. J.; Bilofsky, H. S. Temperature dependence of the proton nuclear magnetic resonance spectra of copper(I) borane complexes, B3H8- salts, and icosahedral carboranes. Quadrupole-induced spin decoupling. Fluxional behavior. *J. Am. Chem. Soc.* **1971**, *93*, 2145−2149.
(44) Beall, H.; Bushweller, C. H.; Dewkett, W. J.; Grace, M. Intramolecular exchange and "thermal" decoupling in B3H8- compounds. *J. Am. Chem. Soc.* **1970**, *92*, 3484−3486.
(45) Chong, M.; Karkamkar, A.; Autrey, T.; Orimo, S.-i.; Jalisatgi, S.; Jensen, C. M. Reversible dehydrogenation of magnesium borohydride to magnesium triborane in the solid state under moderate conditions. *Chem. Commun.* **2011**, *47*, 1330−1332.
(46) Contreras, R.; Wrackmeyer, B. Application of 11B nuclear magnetic resonance spectroscopy to the study of hydroboration-III. 11B Nuclear magnetic resonance study of exchange reactions of triorganyl boranes with borane in tetrahydrofurane and dimethyl sulfide. *Spectrochim. Acta Part A: Mol. Spect.* **1982**, *38*, 941−951.
(47) Greatrex, R.; Greenwood, N. N.; Millikan, M. B.; Rankin, D. W. H.; Robertson, H. E. The molecular structure of hexaborane(12) in the gas phase as determined by electron diffraction. *Dalton Trans.* **1988**, 2335−2339.
(48) Huang, Z.; King, G.; Chen, X.; Hoy, J.; Yisgedu, T.; Lingam, H. K.; Shore, S. G.; Woodward, P. M.; Zhao, J.-C. A Simple and Efficient Way to Synthesize Unsolvated Sodium Octahydrotriborate. *Inorg. Chem.* **2010**, *49*, 8185−8187.
(49) Heřmánek, S. NMR as a tool for elucidation of structures and estimation of electron distribution in boranes and their derivatives. *Inorg. Chim. Acta* **1999**, *289*, 20−44.
(50) Boron NMR Chemical Shifts. 2015, http://www.chemistry.sdsu.edu/research/BNMR (accessed May 20, 2019).
(51) Zhu, T.; Zhang, J. Z. H.; He, X. Automated Fragmentation QM/MM Calculation of Amide Proton Chemical Shifts in Proteins with Explicit Solvent Model. *J. Chem. Theory Comput.* **2013**, *9*, 2104−2114.
(52) Exner, T. E.; Frank, A.; Onila, I.; Möller, H. M. Toward the Quantum Chemical Calculation of NMR Chemical Shifts of Proteins. 3. Conformational Sampling and Explicit Solvents Model. *J. Chem. Theory Comput.* **2012**, *8*, 4818−4827.
(53) Frisch, M. J.; et al. *Gaussian 09*, Revision E.01; Gaussian Inc.: Wallingford CT, 2009.

DOI: 10.1021/acsomega.9b01566
ACS Omega 2019, 4, 12385−12392